X-ray Absorption Studies of the Zn^{2+} Site of Glyoxalase I†

L. Garcia-Iniguez, L. Powers, B. Chance, S. Sellin, B. Mannervik, and A. S. Mildvan*

ABSTRACT: X-ray edge and extended absorption fine structure spectra of Zn^{2+} at the active site of glyoxalase I have been measured. The edge spectrum reveals a simple set of transitions consistent with a 7-coordinate or distorted octahedral Zn^{2+} model complex. Analysis of the fine structure rules out sulfur ligands to Zn^{2+} and yields a best fit complex with Zn^{2+}–N (or Zn^{2+}–O) distances of 2.04 and 2.10 Å, which are too great for tetrahedral Zn^{2+} coordination but are appropriate for an octahedral or more highly coordinated complex. Peaks of electron density in the Fourier-transformed region of the higher order shells at distances of 3–4 Å from the Zn^{2+} are similar to those found with known Zn^{2+}–imidazole model complexes, including carbonic anhydrase [Yachandra, V., Powers, L., & Spiro, T. G. (1983) *J. Am. Chem. Soc. 105*, 6596–6604], indicating at least two imidazole ligands to Zn^{2+} on glyoxalase I. Binding of the heavy atom substrate analogue *S*-(*p*-bromobenzyl)glutathione did not significantly alter the number of atoms directly bonded to Zn^{2+} or their distances. No evidence for coordination of the cysteine sulfur of glutathione by the Zn^{2+} was obtained, and no heavy atom signal from bromine was detected, indicating this atom to be ≥4 Å from the Zn^{2+}. However, conformational changes of the imidazole ligands of Zn^{2+} upon binding of the substrate analogue were suggested by changes in the relative intensity of the doublet peaks at 3–4 Å from the Zn^{2+} and assignable to imidazole. Thus, binding of the substrate analogue in the second coordination sphere may induce a small conformation change in the inner coordination sphere of Zn^{2+}, possibly a rotation of the imidazole ligands.

Glyoxalase I, a dimeric Zn^{2+} metalloenzyme of M_r 23 000 per monomer, is one of two enzymes responsible for the conversion of α-keto aldehydes into α-hydroxy carboxylic acids. The reaction catalyzed is the isomerization of the hemimercaptal adduct between glutathione and methylglyoxal to form the thiol ester:

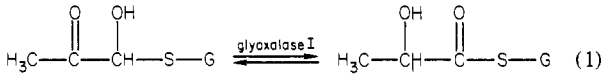

(1)

A metabolic role of the glyoxalase system is believed to be the detoxication of dicarbonyl compounds by converting them to less reactive hydroxy acids (Mannervik, 1981).

Structural studies of the essential metal site of glyoxalase I have heretofore depended upon the replacement of Zn^{2+} with spectroscopically detectable ions such as Co^{2+} or Mn^{2+} (Sellin et al., 1980). Thus, optical and EPR properties of the Co^{2+}-substituted enzyme indicate an octahedral (hexacoordinate) metal complex (Sellin et al., 1983). Water proton relaxation studies with the Mn^{2+}-substituted enzyme have detected two fast-exchanging water ligands on the metal (Sellin et al., 1982a). The effects of the Mn^{2+}- and Co^{2+}-substituted enzymes on nuclear relaxation rates of the product *S*-D-lactoylglutathione have revealed a second-sphere enzyme–metal–(H_2O)–product complex with structural, kinetic, and thermodynamic properties appropriate for the participation of this complex in catalysis (Sellin et al., 1982b; Rosevear et al., 1983). The octahedral geometry about the metal on glyoxalase I is unusual since, as found by X-ray crystallography (Lipscomb, 1980), most other Zn^{2+} metalloenzymes exist as tetrahedral complexes. Octahedral metal coordination has been described for only one other Zn^{2+} metalloenzyme, transcarboxylase, also on the basis of EPR studies of the Co^{2+}-substituted enzyme (Fung et al., 1974).

EXAFS[1] (extended X-ray absorption fine structure) measurements, which do not require crystalline samples, have proven to be useful in determining bond distances, the chemical identity of ligands, and the coordination geometry of active sites in metalloproteins including Zn^{2+} metalloenzymes (Powers, 1982; Yachandra et al., 1983). In this paper, we have used EXAFS to examine the local environment of Zn^{2+} on glyoxalase I directly, without metal replacement, in the absence and presence of a heavy atom substrate analogue.

Experimental Procedures

Materials

Glyoxalase I from human erythrocytes was purified to homogeneity as described by Aronsson et al. (1979), and a mixture of the three isozymes was used. *S*-(*p*-Bromobenzyl)glutathione was prepared by method A of Vince et al. (1971).

Methods

Enzyme Assay. Enzymatic activity was measured by using a spectrophotometric assay with methylglyoxal as the 2-oxaldehyde substrate (Racker, 1951; Marmstål et al., 1979). Protein concentrations were determined by measuring the absorbance at 280 nm [ϵ = 0.80 (mg/mL)$^{-1}$]. The specific activity of the pure enzyme was 1300 units/mg.

† From Bell Telephone Laboratories, Murray Hill, New Jersey 07974 (L.G.-I. and L.P.), the Department of Biochemistry and Biophysics, University of Pennsylvania Medical School, Philadelphia, Pennsylvania 19104 (L.G.-I. and B.C.), the Department of Biochemistry, Arrhenius Laboratory, University of Stockholm, S-10691 Stockholm, Sweden (S.S. and B.M.), and the Department of Physiological Chemistry, Johns Hopkins University School of Medicine, Baltimore, Maryland 21205 (A.S.M.). *Received June 27, 1983.* This work was supported in part by National Institutes of Health Grant HL-18708, Specialized Center of Organized Research (SCOR) Grants HL 15061, GM 27308, GM 27476, and AM 28616, National Science Foundation Grant PCM 8121355, and the Swedish Natural Science Research Council. This is a portion of Stanford Synchotron Radiation Laboratory Project 417B. The work reported herein was performed at SSRL, which is supported by the Office of Basic Energy Sciences, Department of Energy, the Division of Materials Research, National Science Foundation, and the Biotechnology Research Program, Division of Research Resources, National Institutes of Health.

[1] Abbreviations: Tris, tris(hydroxymethyl)aminomethane; TES, 2-[[tris(hydroxymethyl)methyl]amino]ethanesulfonate; EXAFS, extended X-ray absorption fine structure; ImH, imidazole; Py, pyridine; EPR, electron paramagnetic resonance.

0006-2960/84/0423-0685$01.50/0

Sample Preparations. For EXAFS measurements, glyoxalase I was dissolved in 10 mM Tris/TES buffer, pH 6.8, containing 2 mM dithiothreitol and concentrated by vacuum dialysis to a final enzyme-site concentration of 2.0 mM. The Zn^{2+} concentration as determined by atomic absorption spectroscopy was 1.9 ± 0.1 mM. When present, the substrate analogue *S*-(*p*-bromobenzyl)glutathione (2.0 mM) was stoichiometric with the enzyme-site concentration. Because of the low dissociation constant of the glyoxalase I–*S*-(*p*-bromobenzyl)glutathione complex (0.15 μM; Aronsson et al., 1981), the enzyme was 99% saturated with the substrate analogue under these conditions. After the prolonged EXAFS measurements, the samples retained at least 78% of their enzymatic activity.

EXAFS Measurements and Analysis. X-ray absorption measurements were recorded at the Stanford Synchrotron Radiation Laboratory (SSRL) during dedicated operation of the SPEAR storage ring, providing 40–80-mA electron beams at 3.0 GeV (Bienenstock & Winick, 1979). Beam line I-5, which is unfocused and provides ~1 × 10^{10} photons/s with ~1-eV resolution, was used for the zinc-edge and EXAFS measurements. The signal was detected via the fluorescence emitted by the sample with a filter–scintillation counter array (Powers et al., 1981; Chance et al., 1982). A plastic scintillator system placed at 90° to the incident beam recorded the fluorescence intensity from the sample. The samples (0.1 mL) were mounted in lucite holders, which permitted irradiation of the entire sample, covered by mylar films, and inserted in a temperture-regulated N_2 cryostat (Chance et al., 1982).

Protein samples were maintained at −100 °C to ensure no effects from radiation damage (Chance et al., 1980; Powers et al., 1981). Further, the edge spectrum obtained at the end of the measurement period was identical within the error (5%) with that obtained at the beginning, and the successive EXAFS scans showed no detectable changes.

The data were analyzed by procedures previously described (Powers et al., 1981; Brown et al., 1980; Powers, 1982). In the EXAFS analysis, 28 single scans of each protein sample were averaged after they were examined for satisfactory signal to noise ratio, correct edge energy, and the absence of anomalies. Monochromator settings were converted into the corresponding energy values, and the linear background was subtracted from the averaged data set.

The EXAFS modulation of the absorption is given by (Powers, 1982)

$$\chi(k) = -\sum \frac{N_i|f_i(k,\pi)|}{kr_i^2} e^{-2r_i/\lambda(k)} e^{-2\sigma_i^2(k)k^2} \sin\,(2[kr_i + \alpha(k)]) \quad (2)$$

where the sum is taken over the distance r_i from the absorbing atom, N_i is the number of the same type of back-scattering atoms at r_i, $\lambda(k)$ is the photoelectron mean free path, and $f_i(k,\pi)$ is the back-scattering amplitude of the ith atom, which is $\sim Z/k^2$ for $k \gtrsim 4$ Å^{-1}, where Z is the atomic number. The quantity $\sigma(k)$ is the Debye–Waller factor describing the mean square displacement in r_i (from the thermal and lattice disorder), and $\alpha(k)$ is the energy-dependent phase shift of the photoelectron caused by the potentials of both the absorbing and the back-scattering atoms. The magnitude of the photoelectron wave vector k is given by

$$k = [2m_e(E - E_0)]^{1/2}/\hbar \quad (3)$$

where m_e is the electron mass, E is the X-ray energy, and E_0 is the edge energy or threshold energy. The energy was converted to the wave vector, k, and the EXAFS portion, $\chi(k)$, was isolated from the data by a cubic *B*-spline fit to remove the isolated atom or background contribution. The data were then multiplied by k^3 (to remove the approximate $1/k^3$ dependence of the EXAFS above $k \geq 4$ Å^{-1}) and Fourier transformed. Fourier filtering and back-transformation were used to isolate the contribution that each shell makes to the background-corrected EXAFS data.

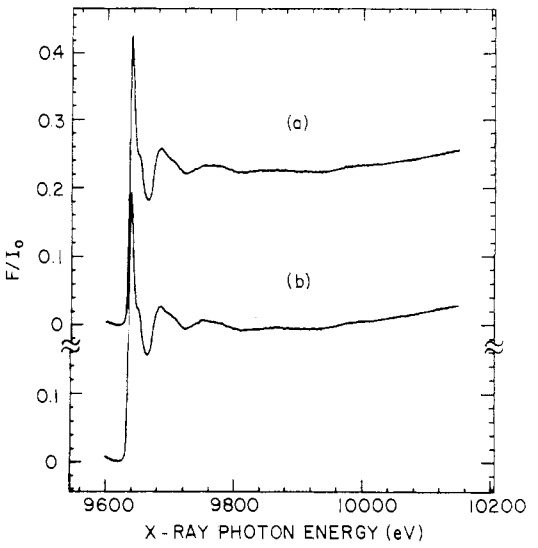

FIGURE 1: X-ray absorption spectra of (a) Zn^{2+}–glyoxalase I and (b) Zn^{2+}–glyoxalase I in the presence of *S*-(*p*-bromobenzyl)glutathione. The linear background has been removed, setting the absorption below the edge to zero. Data were collected by fluorescence, F. I_0 is the incident intensity.

The filtered data of the Zn^{2+} environment on the protein are compared to the amplitude and the phase data of model Zn^{2+} complexes by a nonlinear least-squares fitting program. The fitting program requires four parameters for each type of liganding atom: the average distance, r; the number of scattering atoms, N; the change of the Debye–Waller contribution compared to the model compound, $\Delta\sigma^2$; the change of the edge or threshold compared to the model compound, ΔE_0 (=±2 eV). Significant correlation exists between N and $\Delta\sigma^2$, making the error of N ±20% (Eisenberger & Lengler, 1980). Values of r determined in this manner have an error of ±0.02 Å. Another parameter that is calculated by the fitting program is $\sum^2$, the sum of the residuals squared, which is a measure of the quality of the fit.

Results

EXAFS. The X-ray absorption spectra of the two samples, Zn–glyoxalase I alone and Zn–glyoxalase I in the presence of the heavy atom substrate analogue *S*-(*p*-bromobenzyl)-glutathione (Figure 1), show similar absorption features. Accordingly, the k^3-multiplied, background-subtracted EXAFS data (Figure 2) and their respective Fourier transforms (Figure 3) are also similar.

The EXAFS modulation associated with the innermost shell of atoms is shown in Figure 4. No change in phase is observed when comparing the data from the enzyme alone to those of glyoxalase I in the presence of *S*-(*p*-bromobenzyl)glutathione. The small increase in amplitude observed in the presence of the substrate analogue is within the experimental error.

First Atomic Shell. To determine the metal–ligand distances in the glyoxalase samples, the first-shell data were fitted to the phases and amplitudes obtained from model compounds: $Zn(L\text{-}His)_2 \cdot 2H_2O$, $[(ImH)_4Zn](ClO_4)_2$, $[(ImH)_6Zn]Cl_2$ for Zn^{2+}–N, and Zn–diethyl thiocarbamate for Zn^{2+}–S. The assumption of one or more sulfur ligands to the Zn^{2+} resulted in a poor fit of the data as reflected in a large $\sum^2$ and Zn^{2+}–S

Table I: Bond Combinations for Glyoxalase I

components	metal-ligand distance (Å)[a]	no. of ligands[b]	$\Delta\sigma^2$ ($\times 10^3$)	metal-ligand distance (Å)[a]	no. of ligands[b]	$\Delta\sigma^2$ ($\times 10^3$)	sum of residuals squared (Σ^2)
glyoxalase I	2.07	2	2.36				6.11
	2.04	2	3.02	2.10	2	1.66	3.60
glyoxalase I with	2.07	2	1.26				13.6
S-(*p*-bromobenzyl)glutathione	2.01	2	4.72	2.11	2	5.01	5.31

[a] Error in distance is ~±0.02 Å, but disordered systems have larger errors (±0.03 Å). [b] Total number of nearest-neighbor atoms ± 20%. The ΔE_0 value, the difference in ionization energy of the enzyme vs. that of the model complex $Zn^{2+}(L\text{-His})_2 \cdot 2H_2O$, was small.

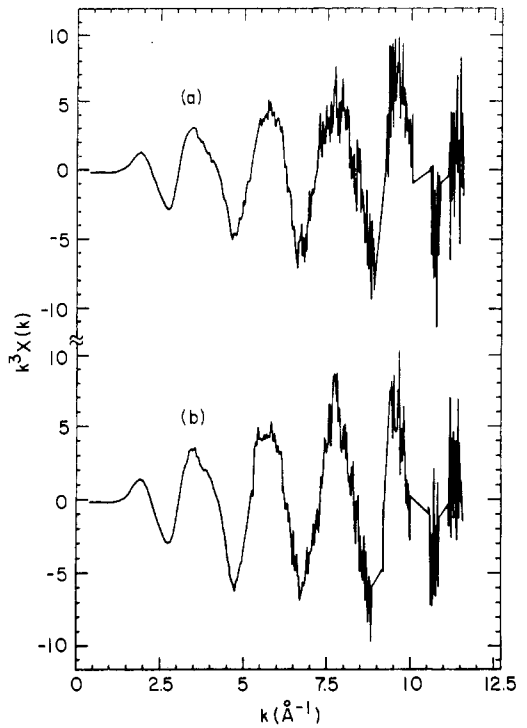

FIGURE 2: EXAFS data. (a) Zn^{2+}–glyoxalase I and (b) Zn^{2+}–glyoxalase I in the presence of *S*-(*p*-bromobenzyl)glutathione spectra, which have had the background removed, were multiplied by k^3 and normalized by division by the edge height.

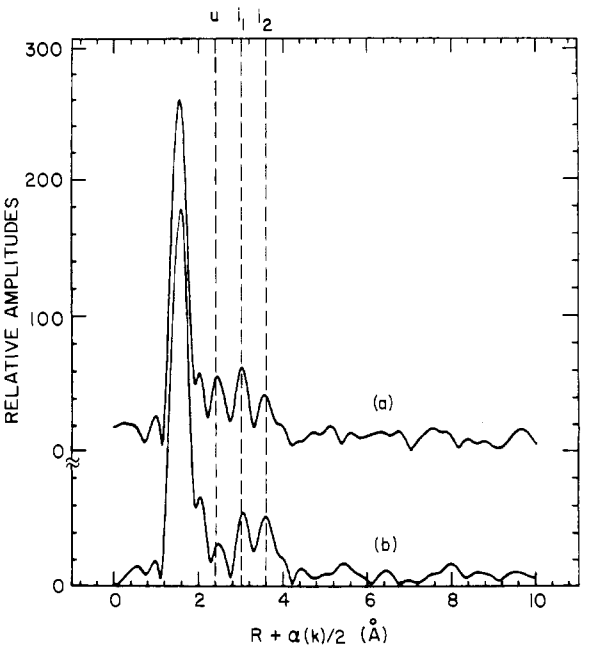

FIGURE 3: Fourier transforms of the $k^3\chi(k)$ data shown in Figure 2 for (a) Zn^{2+}–glyoxalase I and (b) Zn^{2+}–glyoxalase I in the presence of *S*-(*p*-bromobenzyl)glutathione.

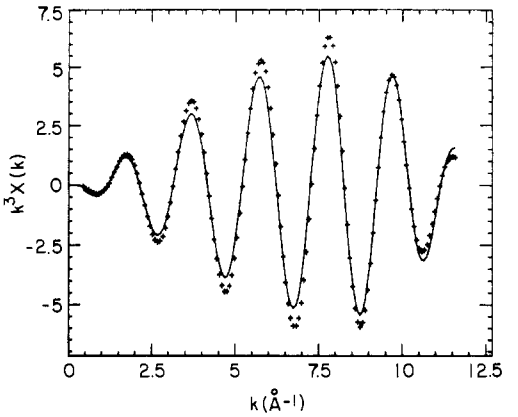

FIGURE 4: First-shell filtered data (window width 1.8–2.0 Å) of Zn^{2+}–glyoxalase I (—) and Zn^{2+}–glyoxalase I in the presence of *S*-(*p*-bromobenzyl)glutathione (+++).

distances of 2.10 Å. These distances are physically much too short for Zn^{2+}–S bonds, which range from 2.331 to 2.815 Å (MacGillavry & Rieck, 1962; Bonamico et al., 1965). Two reasonable solutions involving nitrogen ligands to the Zn^{2+} were obtained for the glyoxalase I samples (Table I). The first is a single atom type fit resulting in two ligands with an average Zn–N (or oxygen) distance of 2.07 ± 0.02 Å. The number of ligands is considerably smaller than expected, but such behavior has been observed for coordination involving a large range of ligand distances or disorder at the site as in amorphous materials (Lee et al., 1981). The second solution allows for two different Zn–N (or oxygen) average distances, resulting in two ligands at 2.04 ± 0.02 Å and two ligands at 2.10 ± 0.02 Å. Disorder may well be present in this structure. Hence, the average distances and coordination numbers may have slightly larger errors than indicated by the quality of the data and the mathematical analysis (Table I). Since the EXAFS data cannot distinguish clearly between N and O (Citrin et al., 1976; Lee et al., 1981), the variation in the Zn^{2+}–ligand distances may be due to one of the ligands being oxygen rather than nitrogen.

Both solutions require Zn–N (or oxygen) distances ≥2.07 Å, suggesting an octahedral Zn^{2+} complex. Distances from Zn^{2+} to nitrogen as great as 2.264 Å have been found in an octahedral complex, while shorter Zn^{2+} nitrogen distances ranging from 1.99 to 2.034 Å are generally found in tetrahedral Zn^{2+}–imidazole complexes (Yachandra et al., 1983).

In the presence of a saturating concentration of *S*-(*p*-bromobenzyl)glutathione (Table I), the solutions are nearly identical with those found in the absence of the substrate analogue, and no significant differences in the number of ligand atoms on Zn^{2+} are detected.

Higher Atomic Shells. Although the first atomic shells are similar in the Fourier-transformed data of glyoxalase I and of the glyoxalase I–analogue complex (Figure 3), the complex exhibits a difference in the relative amplitude of the higher

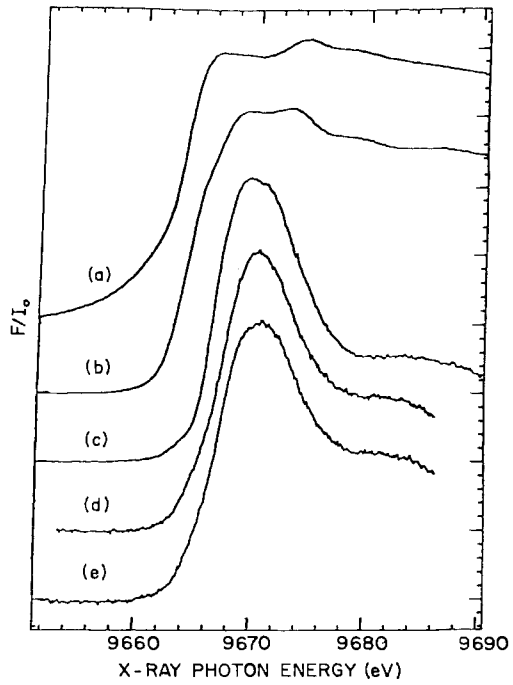

FIGURE 5: X-ray absorption edges of (a) $Zn(ImH)_4(ClO_4)_2$ (i.e., 4-coordinated Zn atom), (b) $(ImH)_6ZnCl_2$ (i.e., 6-coordinated Zn atom), (c) $(Py)_3Zn(NO_3)_2$ (i.e., 7-coordinated Zn atom), (d) glyoxalase I, and (e) glyoxalase I in the presence of *S*-(*p*-bromobenzyl)glutathione.

shells. The peaks at ~3 and ~4 Å labeled i_1 and i_2 (Figure 3) correspond to peaks II and III in the Fourier-transformed data of Zn^{2+}-carbonic anhydrase in which the Zn^{2+} has three imidazole ligands and to such peaks found with several other Zn^{2+}–imidazole model complexes (Yachandra et al., 1983). Hence, these peaks are likely contributions from at least two imidazole ligands on glyoxalase I. When the substrate analogue is bound (Figure 3b), the relative amplitude i_1/i_2 decreases by 28% (with 14% error), suggesting a conformation change in the imidazole ligands. A similar change has been reported in Zn^{2+}–carbonic anhydrase on increasing the pH from 5.5 to 6.9 (Yachandra et al., 1983) and for $(ImH)_4Cu^{2+}SO_4$ and aqueous Cu^{2+}–imidazole (Spiro et al., 1982). The peak labeled u, which also decreases in relative amplitude by 44% when *S*-(*p*-bromobenzyl)glutathione is bound to glyoxalase I (Figure 3b), is also observed in the Zn^{2+}–carbonic anhydrase data (Yachandra et al., 1983). No assignment has been made to this feature since it contains some contribution from the side lobe of the first-shell peak.

The bromine atom of the substrate analogue *S*-(*p*-bromobenzyl)glutathione was not detected in the Zn^{2+} EXAFS. Thus, the analogue binds such that the bromine atom is ≥4 Å from the Zn^{2+} at the catalytic site. Similarly, no evidence for coordination of the sulfur atom of the analogue by the Zn^{2+} was obtained. These results are consistent with nuclear-relaxation studies of the enzyme complex of the product *S*-D-lactoylglutathione, which established a second-sphere complex in which the product atom closest to the metal is the lactoyl carbonyl oxygen at a distance of 4.8 ± 0.3 Å (Sellin et al., 1982b).

Edges. X-ray absorption spectra in the K-edge region contain detailed information on the coordination around the metal since the local electron charge density, i.e., the metal–ligand molecular orbitals, is investigated (Shulman et al., 1976; Powers, 1982). Figure 5 shows the edge spectra of the three types of Zn^{2+} model complexes as well as that of the glyoxalase samples. Comparing the three types of zinc coordination in the model compounds, i.e., $Zn(ImH)_4(ClO_4)_2$ (4-coordinated Zn), $[(ImH)_6Zn]Cl_2$ (6-coordinated Zn), and $(Py)_3Zn(NO_3)_2$ (7-coordinated Zn), to the two glyoxalase I samples, it is found that the edge spectrum of the protein closely resembles the edge spectrum of the 7-coordinated Zn^{2+} compound (Cameron et al., 1972), indicating a distorted octahedral geometry. No change in the edge data is observed on binding of the substrate analogue *S*-(*p*-bromobenzyl)glutathione.

Discussion

Two pieces of evidence from this study indicate distorted octahedral coordination of Zn^{2+} at the active site of glyoxalase I. First, the edge spectrum of the enzyme (Figure 5d) more closely resembles that of a 7-coordinated distorted octahedral Zn^{2+} (Figure 5c) than that of a regular octahedral complex (Figure 5b) and differs greatly from the edge spectrum of tetrahedral complexes where additional features are clearly seen (Figure 5a). Second, the Zn^{2+}–N (or Zn^{2+}–O) distances that were found necessary to fit the EXAFS data (Table I) are greater than those found in tetrahedral or other tetracoordinate Zn^{2+} complexes. They are however appropriate for octahedral or higher Zn^{2+} complexes in which the crowding of ligands precludes short distances (Yachandra et al., 1983; MacGillavry & Rieck, 1962). The present results are in general agreement with EPR and optical spectral studies of the Co^{2+}-substituted enzyme, which indicated octahedral Co^{2+} coordination (Sellin et al., 1983), and with the kinetic observation that the Mg^{2+}-substituted enzyme retains full activity (Sellin et al., 1980) since Mg^{2+} usually forms octahedral complexes (Pauling, 1960). The present results provide independent evidence for this unusual coordination in a Zn^{2+} metalloenzyme. Further, they demonstrate that not only metal-substituted glyoxalase I but also the native Zn^{2+} enzyme has a high coordination number.

The back-scattering from atoms at distances of ~3–4 Å from the Zn^{2+} (Figure 3) when compared with similar results on known Zn^{2+}–imidazole model complexes including carbonic anhydrase (Yachandra et al., 1983) strongly suggests at least two imidazole ligands to Zn^{2+} in glyoxalase I. From the values of Table I, only 70 ± 20% of the expected ligand electron density was detected (Table I). This is not surprising since approximately two of the ligands in Mn^{2+}–glyoxalase are fast-exchanging water molecules (Sellin et al., 1982a,b), which may have high local mobility resulting in sizable Debye–Waller attenuation of the signal. Such attenuation effects have been seen in EXAFS studies of the model complex $(Py)_3Zn^{2+}(NO_3)_2$ (Yachandra et al., 1983) in which the X-ray crystallographic data also show 2–3-fold greater anisotropic temperature factors for the coordinated oxygen atoms of nitrate than for the coordinated nitrogen atoms of pyridine (Cameron et al., 1972). Alternatively, the water (or other) ligands of the metal on glyoxalase I may have escaped detection because the Zn^{2+}–O distances are ≥2.3 Å. It is possible that the peak designated u contains some contributions from such ligands, as well as some side-lobe contributions from the main first-shell peak. However, a similar peak is seen in carbonic anhydrase in which the innermost shell already contains at least four atoms (Yachandra et al., 1983).

The binding of the heavy atom substrate analogue *S*-(*p*-bromobenzyl)glutathione to glyoxalase I does not significantly alter the number of atoms directly bonded to the Zn^{2+} or their distances from the Zn^{2+} (Table I). No evidence for coordination of the cysteine sulfur of glutathione by the Zn^{2+} was obtained, and no heavy atom signal from bromine was detected, indicating this atom to be ≥4 Å from the Zn^{2+}. These results are consistent with nuclear relaxation studies that detected second-sphere product complexes of the Mn^{2+}- and

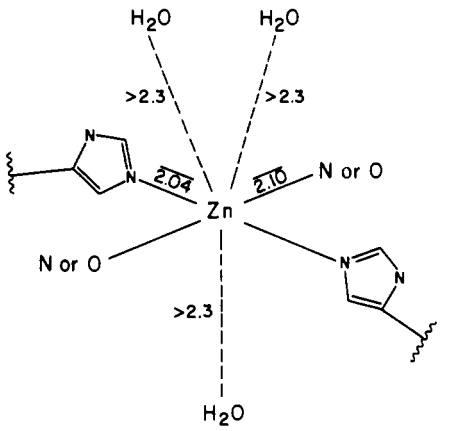

FIGURE 6: Possible coordination geometry of Zn^{2+} at the active site of glyoxalase I based on the model compound $(Py)_3Zn(NO_3)_2$ (Cameron et al., 1972). Average distances for similar ligands are indicated by bars. Errors in distances are given in Table I. Rotation of the imidazole ligands may occur when *S*-(*p*-bromobenzyl)glutathione binds in the second coordination sphere.

Co^{2+}-substituted enzymes (Sellin et al., 1982b; Rosevear et al., 1983). However, possible conformation changes of the two imidazole ligands of Zn^{2+} upon binding of the substrate analogue are suggested in the Fourier-transformed region of the higher order shells by a change in the relative intensity of the peaks at ~3 and ~4 Å, assignable to imidazole (Figure 3). A similar change is seen in these peaks on carbonic anhydrase when the pH is raised from 5.5 to 6.9 (Yachandra et al., 1983) and for $(imidazole)_4Cu^{2+}SO_4$ and aqueous Cu^{2+}–imidazole (Spiro et al., 1982). On both enzymes, these changes might reflect a rotation of the imidazole ligands about their Zn^{2+}–N bonds. Partial quenching of the intrinisic protein fluorescence of glyoxalase I also indicates conformational changes in the protein associated with the binding of *S*-(*p*-bromobenzyl)glutathione (Aronsson et al., 1981).

We conclude that the structure at the Zn^{2+} site of glyoxalase I is a distorted octahedron with two imidazole ligands, two nitrogen or oxygen ligands, and two or three mobile or more distant water ligands (Figure 6). The optical absorption spectrum of Co^{2+}-substituted glyoxalase I (Sellin et al., 1983) has features similar to a Co^{2+} model complex containing two nitrogen and four oxygen ligands (Banci et al., 1982). The binding of the substrate analogue *S*-(*p*-bromobenzyl)glutathione in the second coordination sphere of Zn^{2+} induces a small conformation change in the inner coordination sphere of Zn^{2+}, possibly a rotation of the imidazole ligands.

The mechanism of the glyoxalase I reaction is believed to involve polarization of the carbonyl group of the substrate in the forward reaction and of the product in the reverse reaction (Sellin et al., 1982b). From nuclear-relaxation studies (Sellin et al., 1982b; Rosevear et al., 1983), the carbonyl oxygen of the product is oriented toward the metal but is too far from the metal by 2.4 ± 0.3 Å for direct coordination. Hence, carbonyl polarization by the metal would operate by hydrogen bonding to an intervening ligand, either a water or imidazole ligand or both. The conformational change of the imidazole ligands upon binding of the substrate analogue detected in the EXAFS data may directly or indirectly reflect such interaction of the substrate analogue with the inner sphere ligands. The present results thus support and extend the nuclear-relaxation studies.

Acknowledgments

We thank Y. Ching for his assistance in gathering data on these samples and Professor T. G. Spiro for helpful discussions.

Registry No. Zn, 7440-66-6; glyoxalase I, 9033-12-9; *S*-(*p*-bromobenzyl)glutathione, 31702-37-1.

References

Aronsson, A.-C., Tibbelin, G., & Mannervik, B. (1979) *Anal. Biochem. 92*, 390–393.

Aronsson, A.-C., Sellin, S., Tibbelin, G., & Mannervik, B. (1981) *Biochem. J. 197*, 67–75.

Banci, L., Bencini, A., Benelli, C., Gatteschi, D., & Zanchini, C. (1982) *Struct. Bonding (Berlin) 52*, 37–86.

Beinenstock, A., & Winick, H. (1979) Stanford Synchotron Radiation Laboratory Activity Report No. 79/03:III-2, Stanford University, Stanford, CA.

Bonamico, M., Mazzone, G., Vaciago, A., & Zambonelli, L. (1965) *Acta Crystallogr. 19*, 898–909.

Brown, J. M., Powers, L., Kincaid, B., Larrabee, J. A., & Spiro, T. G. (1980) *J. Am. Chem. Soc. 102*, 4210–4216.

Cameron, A. F., Taylor, D. W., & Nuttall, R. H. (1972) *J. Chem. Soc., Dalton Trans.*, 1603–1608.

Chance, B., Angiolillo, P., Yang, E., & Powers, L. (1980) *FEBS Lett. 112*, 178–182.

Chance, B., Pennie, W., Carman, M., Legallais, V., & Powers, L. (1982) *Anal. Biochem. 124*, 248–257.

Citrin, P. H., Eisenberger, P., & Kincaid, B. M. (1976) *Phys. Rev. Lett. 36*, 1346–1349.

Fung, C.-H., Mildvan, A. S., & Leigh, J. S., Jr. (1974) *Biochemistry 13*, 1160–1169.

Lee, P. A., Citrin, P. H., Eisenberger, P., & Kincaid, B. M. (1981) *Rev. Mod. Phys. 53*, 769–806.

Lipscomb, W. N. (1980) *Adv. Inorg. Biochem. 2*, 273–281.

MacGillavry, C. H., & Rieck, G. D., Eds. (1962) *International Tables for X-ray Crystallography*, Vol. III, p 261, Kynoch Press, Birmingham, England.

Mannervik, B. (1981) in *Enzymatic Basis of Detoxication* (Jakoby, W. B., Ed.) Vol. 2, pp 263–273, Academic Press, New York.

Marmstål, E., Aronsson, A.-C, & Mannervik, B. (1979) *Biochem. J. 183*, 23–30.

Pauling, L. (1960) *The Nature of the Chemical Bond*, pp 250, 533, Cornell University Press, Ithaca, NY.

Powers, L. (1982) *Biochim. Biophys. Acta 683*, 1–38.

Powers, L., Chance, B., Ching, Y., & Angiolillo, P. (1981) *Biophys. J. 34*, 465–498.

Racker, E. (1951) *J. Biol. Chem. 190*, 685–696.

Rosevear, P. R., Chari, R. V. J., Kozarich, J. W., Sellin, S., Mannervik, B., & Mildvan, A. S. (1983) *J. Biol. Chem. 258*, 6823–6826.

Schulman, R. G., Yafet, Y., Eisenberger, P. M., & Blumberg, W. E. (1976) *Proc. Natl. Acad. Sci. U.S.A. 73*, 1384–1388.

Sellin, S., Aronsson, A.-C., & Mannervik, B. (1981) *Acta Chem. Scand., Ser. B 35*, 229–231.

Sellin, S., Eriksson, L. E. G., & Mannervik, B. (1982a) *Biochemistry 21*, 4850–4857.

Sellin, S., Rosevear, P. R., Mannervik, B., & Mildvan, A. S. (1982b) *J. Biol. Chem. 257*, 10023–10029.

Sellin, S., Eriksson, L. E. G., Aronsson, A.-C., & Mannervik, B. (1983) *J. Biol. Chem. 258*, 2091–2093.

Spiro, T. G., Woolery, G. L., Brown, J. M., Powers, L., Winkler, M. E., & Solomon, E. I. (1982) in *Copper Coordination Chemistry: Biochemical and Inorganic Perspectives* (Karlin, K., & Zubieta, J., Eds.) pp 23–41, Adenine Press, New York.

Vince, R., Daluge, S., & Wadd, W. B. (1971) *J. Med. Chem. 14*, 402–404.

Yachandra, V., Powers, L., & Spiro, T. G. (1983) *J. Am. Chem. Soc. 105*, 6596–6604.